

Predicting bacterial growth conditions from mRNA and protein abundances

Mehmet U. Caglar¹, Adam J. Hockenberry¹, Claus O. Wilke^{1,*}

¹Department of Integrative Biology, The University of Texas at Austin, Austin, Texas, USA

*Corresponding author: wilke@austin.utexas.edu

Abstract

Cells respond to changing nutrient availability and external stresses by altering the expression of individual genes. Condition-specific gene expression patterns may [thus](#) provide a promising and low-cost route to quantifying the presence of various small molecules, toxins, or species-interactions in natural environments. However, whether gene expression signatures alone can predict individual environmental growth conditions remains an open question. Here, we used machine learning to predict 16 closely-related growth conditions using 155 datasets of *E. coli* transcript and protein abundances. We show that models are able to discriminate between different environmental features with a relatively high degree of accuracy. We observed a small but significant increase in model accuracy by combining transcriptome and proteome-level data, and we show that [measurements from stationary phase cells typically provide less useful information for discriminating between](#) conditions [as compared to exponentially growing populations](#). Nevertheless, with sufficient training data, gene expression measurements from a single species are capable of distinguishing between environmental conditions that are separated by a single environmental variable.

Formatted: Header

Style Definition: Normal: Font: (Default) Times New Roman

Style Definition: Balloon Text: Font:

Deleted: are typically more difficult

Deleted: distinguish from one another than conditions under exponential growth

Formatted: Header

Introduction

Environmental conditions across the planet vary in terms of their capacity to support microbial life. Individual environments can also change rapidly over time, and these changes are likely to impact the composition of microbial communities and ecosystem functions in unpredictable ways [1,2]. To measure various properties of the environment, microbial cells can be engineered to act as biosensors via rational design of synthetic genetic circuits [3]. In contrast to gold standard approaches that are comparatively labor intensive and expensive, microbial cells can be engineered, for instance, to rapidly screen for the presence of heavy metals in aquatic environments [4]. Such applications can provide a useful, low-cost diagnostic for monitoring environmental changes and detecting pollutants and/or toxins [5], but individual synthetic biology applications take time and resources to develop. Additionally, there is an ever-present concern about potential dangers associated with releasing genetically engineered species into natural environments.

By contrast, prior work has shown that the natural species composition of an environment may be sufficient to serve as a rapid and low-cost biosensor to indicate the presence of various contaminants according to the species abundances identified via meta-genomic sequencing [6–9]. However, many bacterial species within a community are generalists that are capable of thriving in diverse environments and must therefore sense and respond to various environmental signals [10]. For instance, *Escherichia coli* grows inside the comparatively warm, nutrient rich digestive tract of host organisms [11] but spends another portion of its life-cycle exposed to harsh environmental conditions upon being excreted and before finding another host. The mere presence of generalist species in an environment may provide little value for understanding past or current environmental conditions because their gene and expression diversity permits growth across variable environments [12]. The extent to which gene expression patterns of individual generalist species can be used to discriminate between environmental conditions—or to supplement species composition-based methods—remains unknown.

Deleted: Further, individual

Deleted: Microbial species composition is partially indicative of environmental conditions, particularly with regard to the presence of individual specialist species that are well adapted to unique environments [3,4].

Deleted: [5].

Deleted: [6] organisms

Deleted: varied gene expression repertoire permits growth across varied conditions [7].

Gene expression profiles for individual cells or populations contain a wealth of information about their current physiological state, but measurements for thousands of genes across numerous conditions are challenging to integrate under traditional statistical methods. Further, combining different ‘omics’-scale technologies has been shown to provide more valuable information compared to monitoring only mRNA abundances alone, but integrating datasets is challenging due to the biases of individual methods [13] and the inevitability of batch-level effects that occur when datasets are generated across multiple labs and platforms [14,15]. Machine learning methods, by contrast, are frequently applied to such data-rich applications, for example to differentiate between cancerous and normal cells/tissues [16–20] using a variety of different machine learning models [21,22].

In microbiology applications, machine learning has been frequently applied to infer regulatory networks and molecular pathways from gene expression data [23–25], and from this knowledge to predict the growth capabilities of cells in different environments [26–28]. However, the primary focus in many of these studies has been to understand aspects of the cellular physiology. In this framework, environmental change serves as a perturbation that can be used to provide insight into *internal* cellular mechanisms/pathways [29]. While explicitly representing a cell’s internal state may help to predict cellular phenotypes such as growth capabilities across environments [30–32], it is unclear whether explicit representation of cellular metabolic pathways, for instance, are necessary to distinguish between cells growing in different environmental conditions [33,34]. Few studies have focused on using the abundance of cellular macromolecules to predict external environmental features across a range of partially-overlapping conditions and cellular growth states.

Here, we are interested in determining whether gene expression patterns can be leveraged to discriminate between environmental conditions in the absence of prior knowledge about the role and function of individual genes, or explicit representation of

Deleted: On top of their native responses to external conditions, microbial cells can be engineered to act as sensors for a variety of environmental features via rational design of synthetic genetic circuits that may, for instance, cause the cells to fluoresce upon sensing of a particular small molecule [8]. Such applications can provide a useful, low-cost diagnostic for monitoring environmental changes, but individual synthetic biology applications take time and resources to develop. Additionally, there is still a concern about releasing genetically engineered species into natural environments where they may act as low-cost sensors for pollutants or various environmental phenomena of interest [9]. ¶

¶ To partially alleviate this concern, previous work has shown that the species composition of an environment can serve as a rapid and low-cost biosensor to indicate the presence of various contaminants according to the species abundances identified via meta-genomic sequencing [3,10,11]. However, looking at the species composition alone fails to account for the fact that gene expression patterns of individual species—particularly for generalists—may provide even higher resolution into the past and current chemical composition of environments. The extent to which gene expression patterns of individual generalist species can be used to discriminate between environmental conditions remains unknown. ¶

¶ Combining different ‘omics’-scale technologies is likely to provide better discriminatory capability versus only monitoring mRNA abundances, for instance, but integrating datasets is challenging due to the biases of individual methods [12] and the inevitability of batch-level effects that occur when datasets are generated across multiple labs and platforms [13,14]. These problems are further exacerbated when considering the ultimate goal of detecting different environmental conditions *in situ*. ¶

¶ Prior studies have looked into the question of predicting external conditions by using the cells’ internal variables [15,16]. Other studies have interrogated multi-omic datasets from different growth conditions to understand the function of regulatory networks, individual gene functions, and resource allocation strategies [7,17]. However, the main focus of many of these studies has been to understand differences in gene expression patterns across environmental conditions so as to provide insight into *internal* cellular mechanisms and pathways or to predict cellular level phenotypes such as specific growth rates. By contrast, few studies have focused on using the internal state of cells to predict external environmental conditions across a range of partially-overlapping conditions and cellular growth rates. ¶ ... [1]

Deleted: .

Formatted: Header

cellular metabolism. Our study leverages a large dataset of transcriptomic and proteomic measurements of *E.coli* growth under multiple distinct but closely-related conditions [35]. We use mRNA and protein composition data to train several distinct machine learning models and find that highly similar environmental conditions can be discriminated with a high degree of accuracy. We also investigate which conditions are more- and less-challenging to discriminate and find that prediction accuracies decrease for stationary phase cells, indicating the importance of cellular growth for discriminating between conditions. Finally, we caution that the overall accuracy of our models may be limited by training set size; we found that the most difficult conditions to predict are the conditions for which we have the smallest amount of training data. This suggests that our findings may represent a lower bound on the predictive power that is achievable given a greater availability of training data.

Deleted: [18]. We use mRNA and protein composition data to train

Deleted: relatively

Deleted: substantially

Deleted: note

Deleted: our

Deleted: remains

Deleted: such

Deleted: present

Results

Data structure and pipeline design

We used a previously generated dataset of whole-genome *E.coli* (strain REL606) mRNA and protein abundances, measured under 34 different conditions [35,36]. This dataset consists of a total of 155 samples, for which mRNA abundances are available for 152 and protein abundances for 105 (Fig 1). For 102 samples, both mRNA and protein abundances are available. The 34 different experimental conditions were generated by systematically varying four parameters: carbon source, growth phase, Na⁺ concentration, and Mg²⁺ concentration. Here we further simplified the experimental conditions into a total of 16, by grouping similar conditions together (e.g., 100, 200, and 300mM Na⁺ were all labelled as "high Na⁺"). For the remainder of this work (unless otherwise noted) we use the term "growth condition" to refer to the four-dimensional vector of categorical variables defining: i) growth phase (exponential, stationary, late stationary), ii) carbon source (glucose, glycerol, gluconate, lactate), iii) Mg²⁺ concentration (low, base, high), and iv) Na⁺ concentration (base, high). While we note that growth phase is not strictly an environmental feature, we suspected that this

Deleted: coli mRNA and protein abundances, measured under 34 different conditions [18,19]. This dataset consists of a total of 155 samples, for which mRNA abundances are available for 152 and protein abundances for 105 (Fig 1). For 102 samples, both mRNA and protein abundances are available. The 34 different experimental conditions were generated by systematically varying four parameters. Here we further simplified the experimental conditions into a total of 16, by grouping similar conditions together (e.g., 100, 200, and 300mM Na⁺ were all labelled as "high Na⁺"). For the remainder of this manuscript (unless otherwise noted) we use the term "growth condition" to refer to the four-dimensional vector of categorical variables defining growth phase (exponential, stationary, late stationary), carbon source (glucose, glycerol, gluconate, lactate), Mg²⁺ concentration (low, base, high), and Na⁺ concentration (base, high). The question we set out to answer is: to what extent are machine learning models capable of discriminating between these growth parameters given only knowledge of gene expression levels, provided as mRNA abundances, protein abundances, or both

indicator of cellular state would be an important feature to consider since prior research has shown that the macromolecular composition of cells varies substantially between exponentially growing and stationary phase cells [35,36]. With these data and features, the question we set out to answer is: to what extent are machine learning models capable of discriminating between the known growth parameters given only knowledge of gene expression levels?

We first split samples into training/validation and test datasets using a semi-random approach that randomly splits data while preserving class balances. We performed several data processing steps, including batch correction and Principal Component Analysis (PCA), to reduce the dimensionality of the data (see Materials and Methods for details). We analyzed the top 10 genes contributing to the dominant principal components (PC1 and PC2, in both mRNA and protein datasets) and found that they all have orthologs in both B and K strains suggesting that data collection/extrapolation across different strains may not be particularly problematic for future studies (S1 Table). Additionally, PC1 was enriched for highly expressed genes in both mRNA and protein datasets (elongation factors, RNA polymerase subunits, outer membrane proteins, *etc.*), with the protein datasets also consisting of important chaperones (*dnaK* and *groEL*).

During the model tuning phase, we optimized hyperparameters in the machine learning pipeline by further splitting the training/validation data into training and validation sets, fitting models to the labeled training set, and optimizing for model accuracy on the validation set. We performed cross-validation by making 10 unique splits of the training/validation samples—with 75% of samples in training and 25% in validation sets—and searched across a parameter grid to select the hyperparameters that gave the highest F_1 score on the validation set. Finally, we tested the accuracy of model predictions on the test dataset using the optimized hyperparameters from the tuning phase. To assess the overall robustness of our findings, we used repeated testing to replicate our entire pipeline 60 times and report the mean and range of variation in our

Deleted: We applied a general cross-validation strategy and

Deleted: and test datasets. We next used the training data to fit supervised models to the gene expression data to maximize correct

Deleted: of the labeled environmental conditions. At the training stage, we employed parameter tuning, which required a further subdivision of the training data to identify the optimal

Deleted: parameters. Finally, we use the trained and tuned models

Deleted: predict test set data

Deleted: prediction accuracy. To assess robustness of our results to the choice of training and

317 [final test set accuracies](#). Our pipeline is illustrated in Fig 2 and described in [greater](#)
 318 detail in Materials and Methods.
 319

320 **Growth conditions can be predicted accurately from both** 321 **mRNA and protein abundances**

322 After constructing our analysis pipeline, we first asked whether there were major
 323 differences in the performance of different machine learning approaches. [Since our](#)
 324 [overall goal was to demonstrate the feasibility and limitations of using machine learning](#)
 325 [on gene expression data to predict environmental features, we wanted to: i\) ensure that](#)
 326 [our choice of machine learning algorithm did not substantially affect our](#)
 327 [results/conclusions and ii\) determine the best method for this particular application since](#)
 328 [prior work has shown that the choice of machine learning model can substantially affect](#)
 329 [the accuracy of best fitting models \[21,22\]. We tested four different machine learning](#)
 330 [models: three based on Support Vector Machines \(SVMs\) with different kernels \(radial,](#)
 331 [sigmoidal, and linear\) and a fourth using random forest classification. We trained our](#)
 332 [models to predict \[12,37\] the entire four-dimensional condition vector at once for a given](#)
 333 [sample, and used the multi-class macro- \$F_1\$ score \[38\] to quantify prediction accuracy.](#)

334
 335 [We note that various metrics can be applied to quantify model accuracy during](#)
 336 [classification tasks—each with particular strengths and limitations. The multi-class](#)
 337 [macro- \$F_1\$ score is the harmonic mean of precision \(of all the positive predictions made](#)
 338 [by a model, “what fraction are correct?”\) and recall \(of all the possible positive](#)
 339 [predictions, “what fraction does the model return?”\). This quantity approaches zero if](#)
 340 [either quantity approaches zero, and it approaches one if both quantities approach one](#)
 341 [\(representing perfect prediction accuracy\). We further emphasize that our scoring](#)
 342 [scheme will classify a prediction as incorrect if even a single variable is incorrectly](#)
 343 [predicted, even if the predictions for the remaining three variables of interest are](#)
 344 [correct. We made this choice, rather than binary classification of individual variables, so](#)

Formatted: Header

Deleted: data, we repeated this procedure 60 times.

Deleted: the

Deleted: We tested four different machine learning models, three based on Support Vector Machines (SVMs) with different kernels (radial, sigmoidal, and linear) and the fourth using random forest classification. We trained models to predict [7,20] the entire four-dimensional condition vector at once for a given sample, and we used the multi-class macro F_1 score [21] to quantify prediction accuracy. The F_1 score is the harmonic mean of precision and recall. It approaches zero if either quantity approaches zero, and it approaches one if both quantities approach one (representing perfect prediction accuracy). We note that this score is highly conservative as it will classify a prediction as incorrect if a single variable is incorrectly predicted, even if the predictions for the remaining three variables of interest are correct. We assessed model performance during the tuning stage of our pipeline by recording which model had the best F_1 score for each tuning run (S1 and S2 Figs). At the tuning stage, we found that the SVM model with a radial kernel clearly outcompeted the other models when fit to mRNA data, and the random forest model outcompeted the other models when fit to protein data (Table 1).

that our findings would be conservative and represent a lower bound on the prediction accuracy for this task.

We assessed model performance during the tuning stage of our pipeline by recording which model and hyper-parameter set had the best macro- F_1 score for the validation set (S1 and S2 Figs). During this tuning stage, we found that the SVM model with a radial kernel clearly outcompeted the other models when fit to mRNA data, and the random forest model outcompeted the other models when fit to protein data (Table 1).

We next compared the F_1 scores for model predictions applied to the test set. When using mRNA abundance data alone, the distribution of F_1 scores from repeated testing of 60 independent replications were centered around a value of ~ 0.55 (Fig 3). The F_1 score distributions were virtually identical for the three SVM models and was lower for the random forest model. Model performance on test data using only protein abundance measurements was slightly worse than what was achieved with mRNA abundance data. However, it is important to note that the protein abundance data contains fewer samples overall, which may partially explain the decreased predictive accuracy of the protein-only model—a point to which we return to later.

In addition to assessing the overall accuracy of our predictive models using F_1 scores, we also recorded the percentage of times specific growth conditions were accurately or erroneously predicted. We report these results in the form of a confusion matrix (Fig 4). Here, the column headings at the top show the predicted condition from the model on the test set and the rows show the true experimental condition. The numbers and shading in the interior of the matrix represent the percentage of cases that a given experimental condition was predicted to be a certain growth condition (numbers within each row add up to 100). The large numbers/dark colorings along the diagonal highlight the high percentage of true positive predictions whereas any off-diagonal elements represent incorrect predictions. We found that the erroneous off-diagonal predictions are partially driven by the uneven sampling of different conditions in the original dataset.

Formatted: Header

Deleted: our

Deleted: 7

Deleted: were somewhat

Deleted: those

Deleted: conditions

Deleted: power

Deleted: , and we

Deleted: . The

Deleted: .

410 Even though we used sample-number-adjusted class weights in all fitted models, we
411 observed a trend of increasing fractions of correct predictions with increasing number of
412 samples available [during the training stage](#) (S3 Fig).

413
414 As we previously noted, the F_1 score quantifies accuracy by only considering perfect
415 predictions (i.e. when all 4 features are correctly predicted); [a sample that is incorrectly](#)
416 [classified for all four features](#) is thus treated the same as one that only differs from the
417 true set of features by a single incorrect factor. In practice, [however](#), we observed that
418 the majority of incorrect predictions differed from their true condition vector by only a
419 single value (S4 Fig).

421 **Joint consideration of mRNA and protein abundances**

422 **improves model accuracy**

423 We next asked whether predictions could be improved by simultaneously considering
424 [both](#) mRNA and protein abundances. To address this question, we limited our analysis
425 to the subset of 102 samples for which both mRNA and protein abundances were
426 available, and ran our analysis pipeline for mRNA abundances only, protein abundances
427 only, and for the combined dataset containing both mRNA and protein abundances. For
428 all four machine-learning algorithms, protein abundances yielded significantly better
429 predictions than mRNA abundances (Fig 5, Table 2). This is in contrast to Fig 3, where
430 we saw increased accuracy using mRNA abundance data. However, as previously
431 noted, our dataset contains [more](#) mRNA abundance samples, which results in a larger
432 amount of training data [for the results presented in Fig 3](#). When compared on the same
433 exact conditions—as depicted in Fig 5—protein abundance data appears [more valuable](#)
434 for discriminating between different growth conditions. Notably, the combined dataset
435 consisting of both mRNA and protein abundance measurements yielded the best overall
436 predictive accuracy, irrespective of machine-learning algorithm used (Fig 5, Table 2).

Formatted: Header

Deleted: under

Deleted:). A

Deleted: factors

Deleted: ,

Deleted: a larger number

Deleted: .

Deleted: to be

When considering the confusion matrices for the three scenarios (mRNA abundance, protein abundance, and combined), we found that many of the erroneous predictions arising from mRNA abundances alone were not that common when using protein abundances and vice versa (S5 and S6 Figs). For example, when using mRNA abundances, many conditions were erroneously predicted as being exponential phase, glycerol, base Mg^{2+} , base Na^+ ; or as stationary phase, glucose, base Mg^{2+} , high Na^+ ; these particular erroneous predictions were rare or absent when using protein abundances. By contrast, when using protein abundances, several conditions were erroneously predicted as being stationary phase, glycerol, base Mg^{2+} , base Na^+ , and these predictions were virtually absent when using mRNA abundance data. For predictions made from the combined dataset, erroneous predictions unique to either mRNA or protein abundances were suppressed, and only those predictions that arose for both mRNA and protein abundances individually remained present in the combined dataset (S7 Fig).

Prediction accuracy differs between environmental features

We next assessed the sources of inaccuracy in our models. As previously noted, the majority of incorrect predictions differed by only a single factor (S4 Fig). The environmental features that accounted for most of these single incorrect predictions were Mg^{2+} concentration for the protein-only data and carbon source for mRNA-only data. Despite the importance of growth phase to macromolecular abundances, we reasoned that growth (e.g. exponential, stationary, late-stationary) is not an environmental variable and using this as a feature may partially skew our results if the goal is to predict strictly external conditions.

We thus trained and tested separate models using only exponential or only stationary phase datasets and asked to what extent these models could predict the remaining 3 environmental features (carbon source, $[Mg^{2+}]$, and $[Na^+]$). We found that prediction accuracy was consistently better for models trained on exponential-phase samples

Formatted: Header

Deleted: +,

Deleted: generally

Formatted: Font: Italic

Deleted: also

Deleted: .

Deleted: sources

Deleted: Moreover,

Deleted: strictly

481 compared to models trained on stationary-phase samples, irrespective of the machine-
482 learning algorithm used or the data source (mRNA, protein abundances, or both) (Fig
483 6). This observation implies that *E. coli* gene expression patterns during stationary
484 phase are less indicative of the external environment compared to cells experiencing
485 exponential growth. ~~Despite~~ the lower accuracies, however, predictive accuracy from
486 models trained solely on stationary phase cells was still much higher than random
487 expectation, ~~highlighting the fact~~ that quiescent cells retain a unique signature of the
488 external environment for the conditions studied.

Formatted: Header

Deleted: A notable caveat is that we have fewer stationary phase samples and this decrease in accuracy may partially be due to the size of the training dataset. Even despite

Deleted: illustrating

489
490 To better understand which conditions were the most problematic to predict, we
491 constructed models to predict only *individual* features rather than the entire set of 4
492 features. ~~This is an easier task when compared to predicting all 4 dimensions~~
493 ~~simultaneously, and this ease is reflected in the relatively accurate confusion matrices~~
494 ~~that we observed (S8 Fig).~~ For predictions based on mRNA abundances only, models
495 were most accurate in predicting growth phase and least accurate for carbon source,
496 with Mg^{2+} and Na^{+} concentration falling between these two extremes. By contrast, ~~for~~
497 predictions based on protein abundances, the most predictable feature was carbon
498 source, the least predictable was Mg^{2+} concentration, ~~with~~ Na^{+} concentration and growth
499 phase fell in-between these two extremes (Fig 7, S8 Fig). Finally, for the combined
500 mRNA and protein abundance dataset, we found that accuracy for carbon source and
501 Mg^{2+} concentration ~~fell between the accuracies observed using mRNA and protein~~
502 abundances individually. By contrast, accuracies for the Na^{+} concentration and growth
503 phase were ~~as good as—or better than—the prediction accuracies of the individual~~
504 datasets (S9 Fig). Together, these findings highlight that mRNA and protein
505 abundances differ in their ability to discriminate between particular environmental
506 conditions.

Deleted: When making

Deleted: when making

Deleted: , and

Deleted: generally

Deleted: generally

Formatted: Header

Model validation on external data

The samples that we studied throughout this manuscript are fairly heterogeneous and were collected by different individuals over a span of several months/years. However, different sample types were still analyzed within the same labs, by the same protocols, and thus may be more consistent than one might expect from data collected and analyzed independently by different labs—which would be an ultimate goal of future applications of this methodology. We thus applied our best-fitting protein abundance model to analyze protein data with *similar* conditions that was independently collected and analyzed [12]. However, the largest external comparison dataset that we could find consisted of measurements for only ~2,000 proteins, which is substantially less the 4196 proteins that we measured and constructed our models on. Further, the particular bacterial strain (BW25113, a “K” strain) used in this external dataset was distinct from ours (REL606, a “B” strain), so not all of the proteins from our model have direct orthologs in this external dataset. Based on our analysis of the dominant genes contributing to the principal components (S1 Table), however, this strain level-variation may be less important than the missing data values. We tested two alternative approaches of applying our model to the external data. For the first approach, we filled the missing parts of the external data with the median values of our in-house data before making predictions (Table 3). In the second approach, we restricted our training dataset to only include proteins that appeared in the external validation data set (Table 4). These two approaches lead to comparable results. Notably, our model made mostly correct predictions on this *entirely independent* dataset. The model was most accurate at distinguishing between different growth phase data, and moderately accurate at distinguishing Na⁺ concentration and carbon source. The external data did not consist of samples with variable Mg²⁺ concentrations, however, and we note that our model incorrectly predicted several samples to have high Mg²⁺.

Deleted: [7]. Since this external dataset did not contain measurements for all of the 4196 proteins that we measured and constructed our model on, we

Deleted: .

Deleted: .

Deleted: (Fig 8).

Deleted: have variation in

Deleted: levels

Formatted: Font: Helvetica

Discussion

554 Our central goal [here](#) was to determine whether gene expression measurements from a
 555 single species of bacterium are sufficient to predict environmental [features](#). We
 556 analyzed a rich dataset of 152 samples for mRNA data and 105 samples for protein
 557 data across 16 [distinctly classified](#) laboratory conditions as a proof-of-concept. We
 558 [showed](#) that *E. coli* gene expression is responsive to external conditions in a
 559 measurable and consistent way that permits identification of [environmental features](#)
 560 from gene signatures alone [via](#) supervised machine learning techniques.

562 While *E. coli* is a well-characterized species, our analysis relies on none of this *a priori*
 563 knowledge. [Previous approaches have focused on modeling cellular biology and](#)
 564 [metabolism in order to predict the growth capabilities of individual species in various](#)
 565 [environments \[27–29\]. Rather than using varied environmental conditions to interrogate](#)
 566 [cellular regulation \[23,25\], we instead determined that the abundances of cellular](#)
 567 [macromolecules themselves are sufficient to provide accurate information about](#)
 568 [environmental](#) conditions.

570 [Interestingly, we found that consideration of mRNA and protein datasets alone is](#)
 571 [sufficient to produce accurate results, but that joint consideration of both datasets](#)
 572 [results in superior predictive accuracy. This finding implies that post-transcriptional](#)
 573 [regulation is at least partially controlled by external conditions, which has been](#)
 574 [observed by previous studies that have investigated multi-omics datasets \[13,37,39,40\].](#)
 575 [Such regulation may result from post-translational modifications \[41\], stress coping](#)
 576 [mechanisms \[42\], differential translation of mRNAs, or protein-specific degradation](#)
 577 [patterns.](#)

579 [Our results show that cellular growth phase places limits on the predictability of external](#)
 580 [conditions, with stationary phase cells being particularly difficult to distinguish from one](#)
 581 [another irrespective of their external conditions. A possible explanation for this behavior](#)
 582 [may be endogenous metabolism, whereby stationary phase cells start to metabolize](#)
 583 [surrounding dead cells instead of the provided carbon source. This new carbon source,](#)

Formatted: Header

Deleted: in this manuscript

Deleted: growth conditions.

Deleted: distinct

Deleted: could show

Deleted: external conditions

Deleted: using

Deleted: It is thus likely that increasing the number and diversity of training samples and conditions will produce further improvements in accuracy and discrimination between a wider array of

Deleted: Interestingly, we found that consideration of mRNA and protein datasets alone are sufficient to produce accurate results, but that joint consideration of both datasets results in superior predictive accuracy. This finding implies that post-transcriptional regulation is at least partially controlled by external conditions, which has been observed by previous studies that have investigated multi-omics datasets [12,20,22,23]. Such regulation may result from post-translational modifications [24], stress coping mechanisms [25], differential translation of mRNAs, or protein-specific degradation patterns.¶

¶ An important finding that we discovered was that cellular growth phase places limits on the predictability of external conditions, with stationary phase cells being particularly difficult to distinguish from one another irrespective of their external conditions. A possible explanation for this behavior might be associated with endogenous metabolism, whereby stationary phase cells start to metabolize surrounding dead cells instead of the provided carbon source. This new carbon source, which is independent of the externally provided carbon source, may suppress the differences between the cells in different external carbon source environments [26,27]. Another reason for this behavior might be related to strong coupling between gene expression noise and growth rate. Multiple studies have concluded that lower growth rates are associated with higher gene expression noise, which might be a survival strategy in harsh environments [28]. Negative correlations between population average gene expression and noise have been shown for *E. coli* and *Saccharomyces cerevisiae*, lending support for this theory [29,30]. Finally, we note that stationary phase cells have likely depleted the externally supplied carbon sources after several weeks of growth. The similarity of stationary phase cells to other stationary phase cells may be a consequence of them inhabiting more similar chemical environments to one another compared to during exponential growth where nutrient concentrations are more varied across conditions. Nevertheless, discrimination of external environmental factors in stationary phase cells was still much better [2]

which is independent of the externally provided carbon source, may suppress differences between cells growing on different external carbon sources [43,44]. Another reason for this behavior might be related to strong coupling between gene expression noise and growth rate. Multiple studies have concluded that lower growth rates are associated with higher gene expression noise, which might be a survival strategy in harsh environments [45]. Negative correlations between population average gene expression and noise have been shown for *E. coli* and *Saccharomyces cerevisiae*, lending support for this theory [46,47]. Finally, we note that stationary phase cells are likely to have depleted the externally supplied carbon sources after several days of growth. The similarity of stationary phase cells to other stationary phase cells may be a consequence of them actually inhabiting more similar chemical environments to one another compared to during exponential growth where nutrient concentrations are more varied across conditions. Despite these caveats with regard to cellular growth phase, discrimination of external environmental factors in stationary phase cells was still much better than random—indicating that these populations continue to retain information about the external environment despite their overall quiescence.

Another relevant finding to emerge from our study is that different features of the environment may be more or less easy to discriminate from one another and this discrimination may depend on which molecular species is being interrogated. Growth phase, for instance, can be reliably predicted from mRNA concentrations but similar predictions from protein concentrations were less accurate. A possible explanation for this observation may be the differences in life cycles between mRNAs and proteins [36,48]. Given the comparably slow degradation rates of proteins, a large portion of the stationary-phase proteome is likely to have been transcribed during exponential-phase growth. As another example, carbon sources can be reliably predicted from protein concentrations, but the accuracy of carbon source predictions from models trained on mRNA concentrations was more limited. Carbon assimilation is known to be regulated by post-translational regulation [49–51], which may be a possible reason for this finding (Fig 7, S9 Fig).

We investigated over 150 samples spanning 16 unique conditions, but a limitation of our work and conclusions is nevertheless sample size (though our study is comparable to or larger than similar multi-conditional transcriptomic and/or proteomic studies [12,52–54]). The comparison between all available data with the more limited set that includes only the samples for which we have both mRNA and protein abundances indicates that prediction accuracy decreases as the size of our training sets gets smaller (152 vs 102 mRNA samples, Fig 3 compared to Fig 5), strongly implying that training set sizes limit overall model accuracy for at least a portion of our results. A second but related possible issue with our study is associated with sample number bias [55–57]. We made corrections with weight factors [58,59] and used the multi-class macro- F_1 score [60] to account for the fact that some conditions contained more samples than others, but the predictability of *individual* conditions nevertheless increased with the number of training samples for that particular condition (S3 Fig). Accuracy limitations could be more thoroughly evaluated through the use of learning curves to determine whether test set accuracies plateau with increasing training set size, but the class imbalance problem and fairly low number of overall samples per condition in our data make it difficult to evaluate accuracies across a broad range of training set sizes. Future work with larger sample numbers will be useful to interrogate whether accuracies are ultimately limited by training set sizes or by some other features inherent to the data and/or methods.

Another caveat of our study is our choice of score that we used to both optimize hyper-parameters during the training phase and report for our test set accuracies. The most comprehensive and intuitive evaluation of our results is contained within confusion matrices (Fig 4); collapsing these data-rich matrices into a single number is convenient but can also be problematic. Quantifying the accuracy of multi-class classifiers (simultaneously predicting 4 separate vectors) is challenging and standards are generally lacking but the multi-class macro- F_1 score provides an intuitive scale (ranging from 0 to 1, with 1 representing perfect accuracy) and should account for all possible errors by averaging across predictions for each class. We recognize that the use of

other scoring schemes, such as multi-class AUROC [61,62], could alter the model fits during the training phase and the final reported accuracies but the magnitude of these differences should be minor.

We also chose to evaluate different machine learning models throughout this manuscript to ensure the robustness of results and to determine if model choice had a substantial impact on classification accuracy. Overall, we found that the three SVM models performed equivalently to one-another and outperformed random forest models on most tasks. While machine learning models can be difficult to interrogate owing to data transformations, linear kernel SVM models return interpretable output that can be used to determine the most important features and therefore would be preferred for future work in this space given the seeming equivalence between linear, sigmoidal, and radial kernel models. The differences between all models were minor, however, and this finding shows that the accuracy of our classification task is robust to different assumptions.

Our study is a proof-of-principle, demonstrating that gene expression patterns of natural species may provide useful information for assessing various aspects of the environment. Other research has shown that the microbial species composition, derived from meta-genomic sequencing, may be useful for determining the presence of particular contaminants [6]. Our results suggest that further incorporation of species-specific gene expression patterns can likely improve the accuracy of such methods. While genetically engineered strains may play a similar role as low-cost environmental biosensors, we show that—with enough training data—the macromolecular composition of natural populations may provide sufficient information to accurately resolve past and present environmental conditions.

|

Formatted: Header

798 Materials and Methods

799 Data preparation and overall analysis strategy

800 We used a set of 155 *E. coli* samples previously described [35,36]. Throughout this
801 study, we used different subsets of these samples in different parts of the analysis. For
802 “mRNA only” and “protein only” analyses we used all 152 samples with mRNA
803 abundances and all 105 samples with protein abundances, respectively. For
804 performance comparison of machine learning models between mRNA and protein
805 abundances we used the subset of 102 samples that have both mRNA and protein
806 abundance data. After selecting appropriate subsets of the data for a given analysis, we
807 added abundances from technical replicates, normalized abundances by size factors
808 calculated via DeSeq2 [63], and applied a variance stabilizing transformation [64,65]
809 (VST).

Deleted: [18,19].

Deleted: [44]

Field Code Changed

Deleted: 45,46

810
811 For each separate analysis, we divided the data into two subsets, (i) the
812 training/validation set and (ii) the test set, using an 80:20 split (Fig 2). This division was
813 done semi-randomly, such that our algorithm preserved the ratios of different conditions
814 between the training/validation and the test subsets. We retained the condition labels in
815 the training/validation data (thus our learning was supervised) but we discarded the
816 sample labels for the test set. We then applied frozen Surrogate Variable Analysis [66]
817 (fSVA) to remove batch effects from the samples. This algorithm can correct for batch
818 effects in both the training & tune and the test data, without knowing the labels of the
819 test data. After fSVA, we used principal component analysis [67] (PCA) to define the
820 principal axes of the training/validation set and then rotated the test data set with
821 respect to these axes. We then picked the top 10 most significant axes in the
822 training/validation dataset for learning and prediction. Finally, we trained and tuned our
823 candidate machine learning algorithms with the dimension reduced training/validation
824 dataset and then applied those trained and tuned algorithms on the dimension-reduced
825 test dataset to make predictions. This entire procedure was repeated 60 times for each
826 separate analysis (Fig 2).

Deleted: & tune

Deleted: & tune

Deleted: & tune

Deleted: [47]

Deleted: [48] (PCA) to define the principal axes of the training & tune

Deleted: & tune

Deleted: & tune

Formatted: Header

Deleted: [49]

Deleted: [50]

Field Code Changed

Deleted: 51

Deleted: ¶

Model scoring¶

Our goal throughout this work was to predict multiple parameters (i.e., growth phase, carbon source, Mg^{2+} concentration, or Na^+ concentration) of each growth condition at once. Therefore, we could not measure model performance via ROC or precision–recall curves, which assume a simple binary (true/false) prediction. Instead, we assessed prediction accuracy via F_1 scores, which jointly assess precision and recall. In particular, for predictions of multiple conditions at once, we scored prediction accuracy via the multi-class macro F_1 score [21,43,52] that normalizes individual F_1 scores over individual conditions, i.e., it gives each condition equal weight instead of each sample. There are two different macro F_1 score calculation that have been proposed in the literature. First, we can average individual F_1 scores over all conditions i [43]:¶

Deleted: Alternatively, we can average precision and recall and then combine those averages into an F_1 score [21]: ¶

$$F_{1, \text{macro}} = \frac{2 \langle \text{Precision}_i \rangle \langle \text{Recall}_i \rangle}{\langle \text{Precision}_i \rangle + \langle \text{Recall}_i \rangle}.$$
¶

$$F_{1, \text{macro}} = \langle F_{1,i} \rangle$$

$$F_{1,i} = 2 * \text{Precision}_i * \text{Recall}_i / (\text{Precision}_i + \text{Recall}_i).$$

$$F_{1, \text{macro}} = 2 \langle \text{Precision}_i \rangle \langle \text{Recall}_i \rangle / (\langle \text{Precision}_i \rangle + \langle \text{Recall}_i \rangle).$$

890 balances prediction accuracies from different conditions with very different prediction
891 accuracies.

893 Model training and tuning

894 For training, we first divided the training/validation data further into separate training and
895 validation datasets, using a 75:25 split (Fig 2). As before, for the subdivision between
896 training/validation and test data, we did this semi-randomly, while trying to preserve the
897 ratios of individual conditions. We repeated this procedure 10 times to generate 10
898 independent pairs of training and validation datasets. Next, we generated a parameter
899 grid for the tuning process. We optimized the "cost" parameter for all three SVM models
900 and the "gamma" parameter for the SVM models with radial and sigmoidal kernels (S1
901 Fig). For the random forest algorithm, we optimized three parameters; "mtry", "ntrees",
902 and "nodesize".

903
904 We trained each of the four machine learning models on all 10 training datasets and
905 made predictions on the 10 validation datasets. We applied a class weight normalization
906 during training, where class weights are inversely proportional to the corresponding
907 number of training samples and calculated independently for each training run. We
908 calculated macro- F_1 scores for each model parameter setting for each validation
909 dataset and then averaged the scores over all validation datasets to obtain an average
910 performance score for each algorithm and for each parameter combination. The
911 parameter combination with the highest average F_1 score was considered the winning
912 parameter combination and was subsequently used for prediction on the test dataset
913 (Fig 2).

915 Model validation on external data

916 We validated our predictions against independently published external data [12]. This
917 external dataset consisted of 22 conditions, of which we could match five to our

Formatted: Header

Deleted: & tune

Deleted: tuning

Deleted: again

Deleted: ,

Deleted: tuning

Deleted: tuning

Deleted:

Deleted: tuning

Deleted: tuning

Deleted: [7].

928 conditions. For all five samples, Mg^{2+} levels were held constant [in the external dataset](#)
 929 [at a level that](#) *approximately* matched our base Mg^{2+} [concentrations](#). The first sample
 930 used glucose as carbon source, did not experience any osmotic stress (no elevated
 931 sodium), and was collected [during](#) the exponential growth phase. The second sample
 932 used glycerol as carbon source, did not experience any osmotic stress (no elevated
 933 sodium), and was collected in the exponential growth phase. The third sample included
 934 50mM sodium, glucose as carbon source, and was collected in the exponential growth
 935 phase. Because our high-sodium samples all included 100mM of sodium or more [\[35\]](#),
 936 [this third sample fell in-between what we consider “base” sodium and “high” sodium.](#)
 937 Samples four and five used glucose as carbon source, did not experience osmotic
 938 stress, and were measured after 24 and 72 hours of growth, respectively. In our
 939 samples, we defined stationary phase as 24–48 hours and late stationary phase as 1 to
 940 2 weeks [\[35\]](#). Thus, sample four matched our stationary phase samples and sample five
 941 fell in-between our stationary and late-stationary phase samples.

943 Statistical analysis and data availability

944 All statistical analyses were performed in R. All processed data and analysis scripts are
 945 available on GitHub: https://github.com/umutcaglar/ecoli_multiple_growth_conditions
 946 (permanent archived version available via zenodo: 10.5281/zenodo.1294110). mRNA
 947 and protein abundances have been previously published [\[35,36\]](#). Raw Illumina read
 948 data and processed files of read counts per gene are available from the NCBI GEO
 949 database [\[72\]](#) (accession numbers GSE67402 and GSE94117). Mass spectrometry
 950 proteomics data are available via PRIDE [\[73\]](#) (accession numbers PXD002140 and
 951 PXD005721).

Formatted: Header

Deleted: and

Deleted: levels

Formatted: Font: Italic

Deleted: in

Deleted: [18], this third sample fell in-between what we consider base sodium and high sodium.

Deleted: [18].

Deleted: [18,19].

Deleted: [53]

Field Code Changed

Deleted: 54

Acknowledgements

The authors acknowledge support from the Texas Advanced Computing Center (TACC) at The University of Texas at Austin for providing high-performance computing resources.

References

1. Halpern BS, Walbridge S, Selkoe KA, Kappel CV, Micheli F, D'Agrosa C, *et al.* A global map of human impact on marine ecosystems. *Science*. 2008;319: 948–952. doi:10.1126/science.1149345
2. Sahney S, Benton MJ, Ferry PA. Links between global taxonomic diversity, ecological diversity and the expansion of vertebrates on land. *Biol Lett*. 2010;6: 544–547. doi:10.1098/rsbl.2009.1024
3. Slomovic S, Pardee K, Collins JJ. Synthetic biology devices for *in vitro* and *in vivo* diagnostics. *Proc Natl Acad Sci*. 2015;112: 14429–14435. doi:10.1073/pnas.1508521112
4. Bereza-Malcolm LT, Mann G, Franks AE. Environmental sensing of heavy metals through whole cell microbial biosensors: A synthetic biology approach. *ACS Synth Biol*. 2015;4: 535–546. doi:10.1021/sb500286r
5. Roggo C, van der Meer JR. Miniaturized and integrated whole cell living bacterial sensors in field applicable autonomous devices. *Curr Opin Biotechnol*. 2017;45: 24–33. doi:10.1016/j.copbio.2016.11.023
6. He Z, Zhang P, Wu L, Rocha AM, Tu Q, Shi Z, *et al.* Microbial functional gene diversity predicts groundwater contamination and ecosystem functioning. *mBio*. 2018;9: e02435-17. doi:10.1128/mBio.02435-17
7. Poisot T, Kéfi S, Morand S, Stanko M, Marquet PA, Hochberg ME. A continuum of specialists and generalists in empirical communities. *PloS One*. 2015;10: e0114674. doi:10.1371/journal.pone.0114674
8. Flynn TM, Sanford RA, Ryu H, Bethke CM, Levine AD, Ashbolt NJ, *et al.* Functional microbial diversity explains groundwater chemistry in a pristine aquifer. *BMC Microbiol*. 2013;13: 146. doi:10.1186/1471-2180-13-146
9. Hemme CL, Deng Y, Gentry TJ, Fields MW, Wu L, Barua S, *et al.* Metagenomic insights into evolution of a heavy metal-contaminated groundwater microbial community. *ISME J*. 2010;4: 660–672. doi:10.1038/ismej.2009.154
10. Sriswasdi S, Yang C, Iwasaki W. Generalist species drive microbial dispersion and evolution. *Nat Commun*. 2017;8: 1162. doi:10.1038/s41467-017-01265-1

Formatted: Font: Not Bold

- Deleted: 1. —Halpern BS, Walbridge S, Selkoe KA, Kappel CV, Micheli F, D'Agrosa C, *et al.* A global map of human impact on marine ecosystems. *Science*. 2008;319: 948–952. doi:10.1126/science.1149345
2. —Sahney S, Benton MJ, Ferry PA. Links between global taxonomic diversity, ecological diversity and the expansion of vertebrates on land. *Biol Lett*. 2010;6: 544–547. doi:10.1098/rsbl.2009.1024
3. —He Z, Zhang P, Wu L, Rocha AM, Tu Q, Shi Z, *et al.* Microbial Functional Gene Diversity Predicts Groundwater Contamination and Ecosystem Functioning. *mBio*. 2018;9: e02435-17. doi:10.1128/mBio.02435-17
4. —Poisot T, Kéfi S, Morand S, Stanko M, Marquet PA, Hochberg ME. A continuum of specialists and generalists in empirical communities. *PloS One*. 2015;10: e0114674. doi:10.1371/journal.pone.0114674
5. —Sriswasdi S, Yang C, Iwasaki W. Generalist species drive microbial dispersion and evolution. *Nat Commun*. 2017;8: 1162. doi:10.1038/s41467-017-01265-1
6. —Mitchell A, Romano GH, Groisman B, Yona A, Dekel E, Kupiec M, *et al.* Adaptive prediction of environmental changes by microorganisms. *Nature*. 2009;460: 220–224. doi:10.1038/nature08112
7. —Schmidt A, Kochanowski K, Vedelaar S, Ahrné E, Volkmer B, Callipo L, *et al.* The quantitative and condition-dependent *Escherichia coli* proteome. *Nat Biotechnol*. 2016;34: 104–110. doi:10.1038/nbt.3418
8. —Slomovic S, Pardee K, Collins JJ. Synthetic biology devices for *in vitro* and *in vivo* diagnostics. *Proc Natl Acad Sci*. 2015;112: 14429–14435. doi:10.1073/pnas.1508521112
9. —Roggo C, van der Meer JR. Miniaturized and integrated whole cell living bacterial sensors in field applicable autonomous devices. *Curr Opin Biotechnol*. 2017;45: 24–33. doi:10.1016/j.copbio.2016.11.023
10. —Flynn TM, Sanford RA, Ryu H, Bethke CM, Levine AD, Ashbolt NJ, *et al.* Functional microbial diversity explains groundwater chemistry in a pristine aquifer. *BMC Microbiol*. 2013;13: 146. doi:10.1186/1471-2180-13-146
11. —Hemme CL, Deng Y, Gentry TJ, Fields MW, Wu L, Barua S, *et al.* Metagenomic insights into evolution of a heavy metal-contaminated groundwater microbial community. *ISME J*. 2010;4: 660–672. doi:10.1038/ismej.2009.154
12. —Kim M, Rai N, Zorraqino V, Tagkopoulou I. Multi-omics integration accurately predicts cellular state in unexplored conditions for *Escherichia coli*. *Nat Commun*. 2016;7. doi:10.1038/ncomms13090
13. —Leek JT, Scharpf RB, Bravo HC, Simcha D, Langmead B, Johnson WE, *et al.* Tackling the widespread and critical impact of batch effects in ... [3]

11. [Mitchell A, Romano GH, Groisman B, Yona A, Dekel E, Kupiec M, *et al.* Adaptive prediction of environmental changes by microorganisms. *Nature*. 2009;460: 220–224. doi:10.1038/nature08112](#)
12. [Schmidt A, Kochanowski K, Vedelaar S, Ahrné E, Volkmer B, Callipo L, *et al.* The quantitative and condition-dependent *Escherichia coli* proteome. *Nat Biotechnol*. 2016;34: 104–110. doi:10.1038/nbt.3418](#)
13. [Kim M, Rai N, Zorraqino V, Tagkopoulos I. Multi-omics integration accurately predicts cellular state in unexplored conditions for *Escherichia coli*. *Nat Commun*. 2016;7. doi:10.1038/ncomms13090](#)
14. [Leek JT, Scharpf RB, Bravo HC, Simcha D, Langmead B, Johnson WE, *et al.* Tackling the widespread and critical impact of batch effects in high-throughput data. *Nat Rev Genet*. 2010;11. doi:10.1038/nrg2825](#)
15. [Scharpf RB, Ruczinski I, Carvalho B, Doan B, Chakravarti A, Irizarry RA. A multilevel model to address batch effects in copy number estimation using SNP arrays. *Biostatistics*. 2011;12: 33–50. doi:10.1093/biostatistics/kxq043](#)
16. [Ramaswamy S, Tamayo P, Rifkin R, Mukherjee S, Yeang C-H, Angelo M, *et al.* Multiclass cancer diagnosis using tumor gene expression signatures. *Proc Natl Acad Sci*. 2001;98: 15149–15154. doi:10.1073/pnas.211566398](#)
17. [Nguyen DV, Rocke DM. Multi-class cancer classification via partial least squares with gene expression profiles. *Bioinformatics*. 2002;18: 1216–1226. doi:10.1093/bioinformatics/18.9.1216](#)
18. [Nguyen DV, Rocke DM. Tumor classification by partial least squares using microarray gene expression data. *Bioinformatics*. 2002;18: 39–50. doi:10.1093/bioinformatics/18.1.39](#)
19. [Lee Y, Lee C-K. Classification of multiple cancer types by multicategory support vector machines using gene expression data. *Bioinformatics*. 2003;19: 1132–1139. doi:10.1093/bioinformatics/btg102](#)
20. [Furey TS, Cristianini N, Duffy N, Bednarski DW, Schummer M, Haussler D. Support vector machine classification and validation of cancer tissue samples using microarray expression data. *Bioinformatics*. 2000;16: 906–914. doi:10.1093/bioinformatics/16.10.906](#)
21. [Statnikov A, Aliferis CF, Tsamardinos I, Hardin D, Levy S. A comprehensive evaluation of multicategory classification methods for microarray gene expression cancer diagnosis. *Bioinformatics*. 2005;21: 631–643. doi:10.1093/bioinformatics/bti033](#)
22. [Statnikov A, Wang L, Aliferis CF. A comprehensive comparison of random forests and support vector machines for microarray-based cancer classification. *BMC Bioinformatics*. 2008;9: 319. doi:10.1186/1471-2105-9-319](#)

23. [Bonneau R, Reiss DJ, Shannon P, Facciotti M, Hood L, Baliga NS, *et al.* The Inferelator: an algorithm for learning parsimonious regulatory networks from systems-biology data sets *de novo*. Genome Biol. 2006;7: R36. doi:10.1186/gb-2006-7-5-r36](#)
24. [Bansal M, Belcastro V, Ambesi-Impombato A, di Bernardo D. How to infer gene networks from expression profiles. Mol Syst Biol. 2007;3. doi:10.1038/msb4100120](#)
25. [Faith JJ, Hayete B, Thaden JT, Mogno I, Wierzbowski J, Cottarel G, *et al.* Large-scale mapping and validation of *Escherichia coli* transcriptional regulation from a compendium of expression profiles. PLoS Biol. 2007;5: e8. doi:10.1371/journal.pbio.0050008](#)
26. [Bonneau R, Facciotti MT, Reiss DJ, Schmid AK, Pan M, Kaur A, *et al.* A predictive model for transcriptional control of physiology in a free living cell. Cell. 2007;131: 1354–1365. doi:10.1016/j.cell.2007.10.053](#)
27. [Chandrasekaran S, Price ND. Probabilistic integrative modeling of genome-scale metabolic and regulatory networks in *Escherichia coli* and *Mycobacterium tuberculosis*. Proc Natl Acad Sci. 2010;107: 17845–17850. doi:10.1073/pnas.1005139107](#)
28. [Carrera J, Estrela R, Luo J, Rai N, Tsoukalas A, Tagkopoulos I. An integrative, multi-scale, genome-wide model reveals the phenotypic landscape of *Escherichia coli*. Mol Syst Biol. 2014;10: 735–735. doi:10.15252/msb.20145108](#)
29. [Machado D, Herrgård M. Systematic evaluation of methods for integration of transcriptomic data into constraint-based models of metabolism. PLoS Comput Biol. 2014;10: e1003580. doi:10.1371/journal.pcbi.1003580](#)
30. [Brandes A, Lun DS, Ip K, Zucker J, Colijn C, Weiner B, *et al.* Inferring carbon sources from gene expression profiles using metabolic flux models. PLoS One. 2012;7: e36947. doi:10.1371/journal.pone.0036947](#)
31. [Sridhara V, Meyer AG, Rai P, Barrick JE, Ravikumar P, Segrè D, *et al.* Predicting growth conditions from internal metabolic fluxes in an *in-silico* model of *E. coli*. PLoS One. 2014;9: e114608. doi:10.1371/journal.pone.0114608](#)
32. [Hui S, Silverman JM, Chen SS, Erickson DW, Basan M, Wang J, *et al.* Quantitative proteomic analysis reveals a simple strategy of global resource allocation in bacteria. Mol Syst Biol. 2015;11: 784. doi:10.15252/msb.20145697](#)
33. [Airoidi EM, Huttenhower C, Gresham D, Lu C, Caudy AA, Dunham MJ, *et al.* Predicting cellular growth from gene expression signatures. PLoS Comput Biol. 2009;5: e1000257. doi:10.1371/journal.pcbi.1000257](#)
34. [Gutteridge A, Pir P, Castrillo JI, Charles PD, Lilley KS, Oliver SG. Nutrient control of eukaryote cell growth: a systems biology study in yeast. BMC Biol. 2010;8: 68. doi:10.1186/1741-7007-8-68](#)

35. Caglar MU, Houser JR, Barnhart CS, Boutz DR, Carroll SM, Dasgupta A, *et al.* The *E. coli* molecular phenotype under different growth conditions. *Sci Rep.* 2017;7: 45303. doi:10.1038/srep45303
36. Houser JR, Barnhart C, Boutz DR, Carroll SM, Dasgupta A, Michener JK, *et al.* Controlled measurement and comparative analysis of cellular components in *E. coli* reveals broad regulatory changes in response to glucose starvation. *PLoS Comput Biol.* 2015;11: e1004400. doi:10.1371/journal.pcbi.1004400
37. Wilmes A, Limonciel A, Aschauer L, Moenks K, Bielow C, Leonard MO, *et al.* Application of integrated transcriptomic, proteomic and metabolomic profiling for the delineation of mechanisms of drug induced cell stress. *J Proteomics.* 2013;79: 180–194. doi:10.1016/j.jprot.2012.11.022
38. Sokolova M, Lapalme G. A systematic analysis of performance measures for classification tasks. *Inf Process Manag.* 2009;45: 427–437. doi:10.1016/j.ipm.2009.03.002
39. Nie L, Wu G, Culley DE, Scholten JCM, Zhang W. Integrative analysis of transcriptomic and proteomic data: challenges, solutions and applications. *Crit Rev Biotechnol.* 2007;27: 63–75. doi:10.1080/07388550701334212
40. Zhang W, Li F, Nie L. Integrating multiple “omics” analysis for microbial biology: application and methodologies. *Microbiology.* 2010;156: 287–301. doi:10.1099/mic.0.034793-0
41. Oliveira AP, Sauer U. The importance of post-translational modifications in regulating *Saccharomyces cerevisiae* metabolism. *FEMS Yeast Res.* 2012;12: 104–117. doi:10.1111/j.1567-1364.2011.00765.x
42. de Nadal E, Ammerer G, Posas F. Controlling gene expression in response to stress. *Nat Rev Genet.* 2011;12: 833–845. doi:10.1038/nrg3055
43. Kolter R, Siegele DA, Tormo A. The stationary phase of the bacterial life cycle. *Annu Rev Microbiol.* 1993;47: 855–874. doi:10.1146/annurev.mi.47.100193.004231
44. Maier RM, Pepper IL. Chapter 3 - Bacterial Growth. *Environmental Microbiology* (Third edition). San Diego: Academic Press; 2015. pp. 37–56. doi:10.1016/B978-0-12-394626-3.00003-X
45. Keren L, van Dijk D, Weingarten-Gabbay S, Davidi D, Jona G, Weinberger A, *et al.* Noise in gene expression is coupled to growth rate. *Genome Res.* 2015; gr.191635.115. doi:10.1101/gr.191635.115
46. Bar-Even A, Paulsson J, Maheshri N, Carmi M, O’Shea E, Pilpel Y, *et al.* Noise in protein expression scales with natural protein abundance. *Nat Genet.* 2006;38: 636–643. doi:10.1038/ng1807

- 1229 47. Taniguchi Y, Choi PJ, Li G-W, Chen H, Babu M, Hearn J, *et al.* Quantifying *E. coli*
1230 proteome and transcriptome with single-molecule sensitivity in single cells. *Science*.
1231 2010;329: 533–538. doi:10.1126/science.1188308
- 1232 48. Milo R, Jorgensen P, Moran U, Weber G, Springer M. BioNumbers—the database of key
1233 numbers in molecular and cell biology. *Nucleic Acids Res*. 2010;38:D750-D753.
1234 doi:10.1093/nar/gkp889
- 1235 49. Martínez-Gómez K, Flores N, Castañeda HM, Martínez-Batallar G, Hernández-Chávez G,
1236 Ramírez OT, *et al.* New insights into *Escherichia coli* metabolism: carbon scavenging,
1237 acetate metabolism and carbon recycling responses during growth on glycerol. *Microb Cell*
1238 *Factories*. 2012;11: 46. doi:10.1186/1475-2859-11-46
- 1239 50. Perrenoud A, Sauer U. Impact of global transcriptional regulation by ArcA, ArcB, Cra, Crp,
1240 Cya, Fnr, and Mlc on glucose catabolism in *Escherichia coli*. *J Bacteriol*. 2005;187: 3171–
1241 3179. doi:10.1128/JB.187.9.3171-3179.2005
- 1242 51. Kumar R, Shimizu K. Transcriptional regulation of main metabolic pathways of *cyoA*,
1243 *cydB*, *fnr*, and *fur* gene knockout *Escherichia coli* in C-limited and N-limited aerobic
1244 continuous cultures. *Microb Cell Factories*. 2011;10: 3. doi:10.1186/1475-2859-10-3
- 1245 52. Soufi B, Krug K, Harst A, Macek B. Characterization of the *E. coli* proteome and its
1246 modifications during growth and ethanol stress. *Front Microbiol*. 2015;6: 103.
1247 doi:10.3389/fmicb.2015.00103
- 1248 53. Lewis NE, Cho B-K, Knight EM, Palsson BO. Gene expression profiling and the use of
1249 genome-scale *in silico* models of *Escherichia coli* for analysis: providing context for
1250 content. *J Bacteriol*. 2009;191: 3437–3444. doi:10.1128/JB.00034-09
- 1251 54. Yoon SH, Han M-J, Jeong H, Lee CH, Xia X-X, Lee D-H, *et al.* Comparative multi-omics
1252 systems analysis of *Escherichia coli* strains B and K-12. *Genome Biol*. 2012;13: R37.
1253 doi:10.1186/gb-2012-13-5-r37
- 1254 55. Batista GEAPA, Prati RC, Monard MC. A study of the behavior of several methods for
1255 balancing machine learning training data. *ACM SIGKDD Explor Newsl*. 2004;6: 20–29.
1256 doi:10.1145/1007730.1007735
- 1257 56. Chawla NV. Data mining for imbalanced datasets: An overview. In: *Data Mining and*
1258 *Knowledge Discovery Handbook*. Springer US; 2005. pp. 853–867. doi:10.1007/0-387-
1259 25465-X_40
- 1260 57. He H, Garcia EA. Learning from imbalanced data. *IEEE Trans Knowl Data Eng*. 2009;21:
1261 1263–1284. doi:10.1109/TKDE.2008.239
- 1262 58. Huang Y-M, Du S-X. Weighted support vector machine for classification with uneven
1263 training class sizes. 2005 *International Conference on Machine Learning and Cybernetics*.
1264 2005;7:4365-4369 doi:10.1109/ICMLC.2005.1527706

- 1265 59. Support Vector Machines [Internet]. [cited 24 Apr 2017]. Available:
1266 <http://www.di.fc.ul.pt/~jpn/r/svm/svm.html>
- 1267 60. Yang Y. An evaluation of statistical approaches to text categorization. *Inf Retr.* 1999;1: 69–
1268 90. doi:10.1023/A:1009982220290
- 1269 61. Hand DJ, Till RJ. A simple generalisation of the Area Under the ROC Curve for multiple
1270 class classification problems. *Mach Learn.* 2001;45: 171–186.
- 1271 62. Landgrebe TCW, Duin RPW. Approximating the multiclass ROC by pairwise analysis.
1272 *Pattern Recognit Lett.* 2007;28: 1747–1758. doi:10.1016/j.patrec.2007.05.001
- 1273 63. Love MI, Huber W, Anders S. Moderated estimation of fold change and dispersion for
1274 RNA-seq data with DESeq2. *Genome Biol.* 2014;15: 550. doi:10.1186/s13059-014-0550-8
- 1275 64. Differential analysis of count data – the DESeq2 package [Internet]. 27 Jun 2016 [cited 12
1276 Apr 2016]. Available:
1277 <http://www.bioconductor.org/packages//2.13/bioc/vignettes/DESeq2/inst/doc/DESeq2.pdf>
- 1278 65. Anders S, Huber W. Differential expression analysis for sequence count data. *Genome Biol.*
1279 2010;11: R106. doi:10.1186/gb-2010-11-10-r106
- 1280 66. Parker HS, Bravo HC, Leek JT. Removing batch effects for prediction problems with
1281 frozen surrogate variable analysis. *PeerJ.* 2014;2: e561. doi:10.7717/peerj.561
- 1282 67. Jolliffe I. Principal Component Analysis. Wiley StatsRef: Statistics Reference Online. John
1283 Wiley & Sons, Ltd; 2014. doi:10.1002/9781118445112.stat06472
- 1284 68. Meyer D, Wien TU. Support Vector Machines. The interface to libsvm in package e1071.
1285 Online-Documentation of the package e1071 for “R. 2001.
- 1286 69. Liaw A, Wiener M. Classification and regression by randomForest. *R News.* 2002;2: 18–
1287 22.
- 1288 70. Chang C-C, Lin C-J. LIBSVM: a library for support vector machines. *ACM Trans Intell*
1289 *Syst Technol.* 2011;2: 27:1–27:27. doi:10.1145/1961189.1961199
- 1290 71. Ghamrawi N, McCallum A. Collective multi-label classification. *Proceedings of the 14th*
1291 *ACM International Conference on Information and Knowledge Management.* 2005;195–
1292 200. doi:10.1145/1099554.1099591
- 1293 72. Barrett T, Wilhite SE, Ledoux P, Evangelista C, Kim IF, Tomashevsky M, *et al.* NCBI
1294 GEO: archive for functional genomics data sets—update. *Nucleic Acids Res.* 2013;41:
1295 D991–D995. doi:10.1093/nar/gks1193
- 1296 73. Vizcaíno JA, Deutsch EW, Wang R, Csordas A, Reisinger F, Ríos D, *et al.*
1297 ProteomeXchange provides globally coordinated proteomics data submission and
1298 dissemination. *Nature Biotechnol.* 2014;32:223–226. doi:10.1038/nbt.2839

|

1299

Formatted: Header

Figures

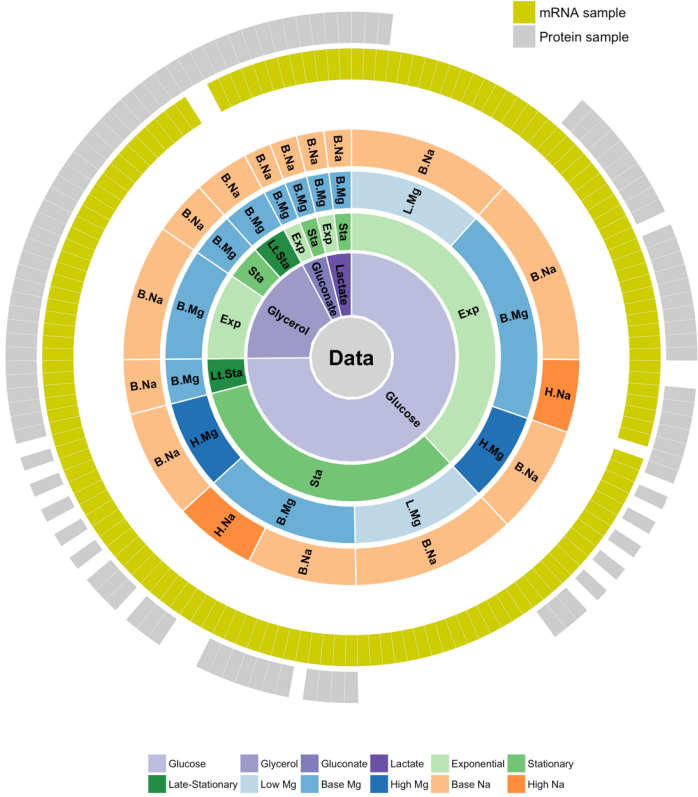
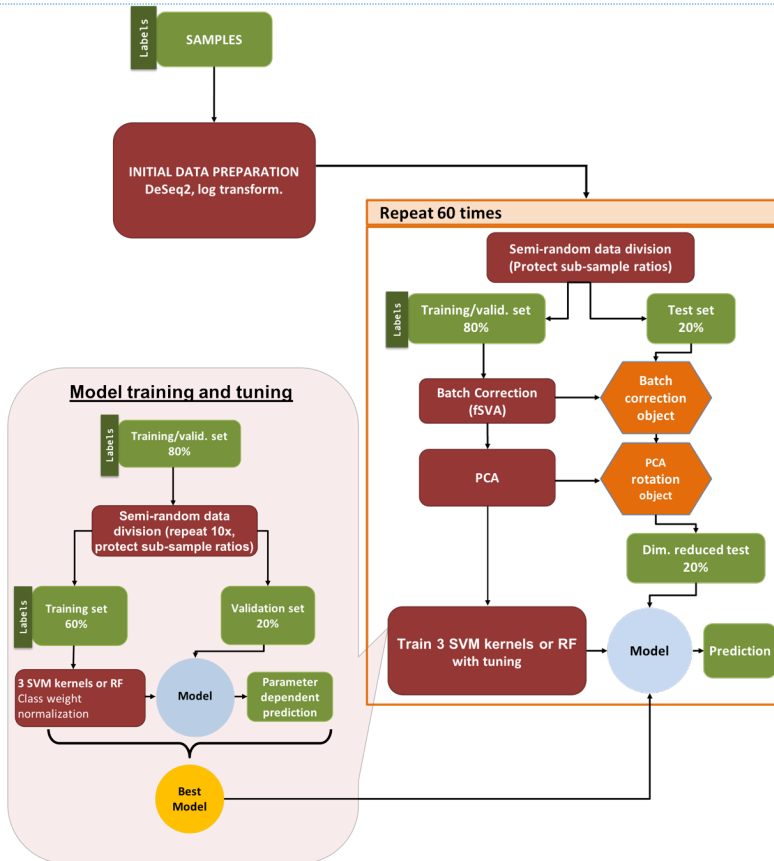


Figure 1: Overview of available gene expression data. Our study uses a previously published dataset consisting of 155 samples [13, 14]. 152 samples have whole-transcriptome RNA-seq reads and 105 have mass-spec proteomics reads. 102 of the 155 samples have both mRNA and protein reads. Bacteria were grown on four different carbon sources (glucose, glycerol, gluconate, and lactate), two sodium concentrations (base and high), and three magnesium concentrations (low, base, and high). Samples were taken at multiple time points during a two-week interval, and they can be broadly subdivided into exponential phase, stationary phase, and late stationary phase samples.

|

1312



1313 **Figure 2: Machine learning pipeline.** Our pipeline can be separated into three parts:
 1314 (i) initial data preparation, (ii) training and prediction, and (iii) model tuning. After (i)
 1315 initial data preparation, the samples are (ii) semi-randomly (preserving sub-sample
 1316 ratios) separated into 2 parts, the training/validation set and the test set. After applying
 1317 fSVA and PCA to the training/validation data, we train supervised SVM or random forest
 1318 models on the training/validation set. After obtaining the tuned model we make
 1319 predictions on the test data that has been batch corrected (via fSVA) and rotated (via
 1320 PCA). This whole process is repeated 60 times to collect statistics on model
 1321 performance. For model tuning (iii), the training/validation data set is similarly divided
 1322 semi-randomly into training and validation datasets to optimize hyperparameters using a
 1323 grid search approach. The tuning procedure is repeated 10 times and the parameter set
 1324 that performs best, on average, during the 10 repeats is considered the winning
 1325 model and is used for prediction on the test set data.

Formatted: Header

Deleted: <object>

Deleted: & tune

Deleted: via tuning

Deleted: & tune

Deleted: tune

Deleted: .

Deleted: model

Deleted:

Deleted:

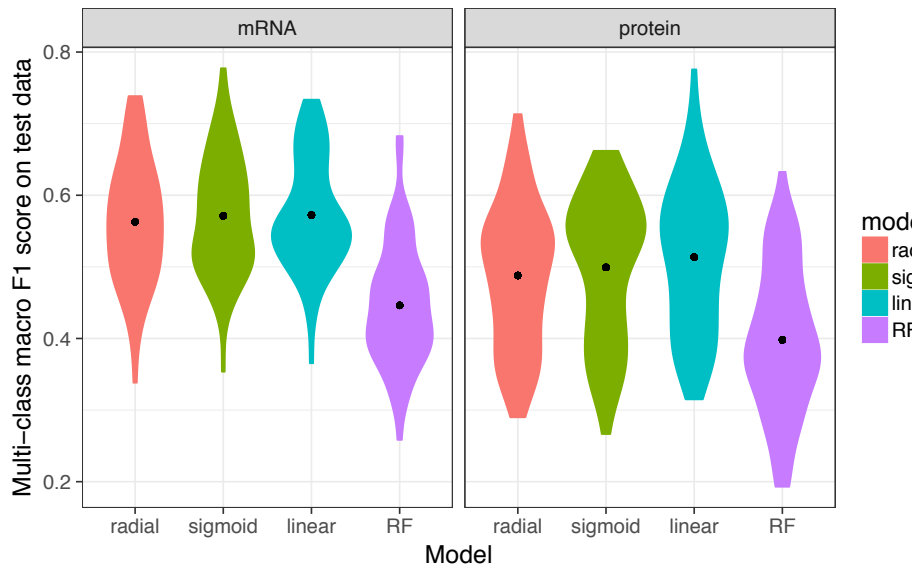


Figure 3: Performance of multi-class predictions. Distributions of multi-class macro F_1 score for prediction of growth conditions from mRNA or protein abundances, using four different machine-learning algorithms (SVM with radial, sigmoidal, or linear kernel, and random forest [RF] models). For each model type, 60 independent models were trained on 60 independent subdivisions of the data into training/validation and test sets. We found that random forest models consistently performed worse than SVM models, and predictions based on mRNA data were slightly better than predictions based on protein data. The black dots represent the mean F_1 scores.



Figure 4. Test set prediction accuracy for specific growth conditions. In each matrix, rows represent true conditions and columns represent predicted conditions. The numbers in the cells and the shading of the cells represent the percentage (out of 60 independent replicates) with which a given true condition is predicted as a certain predicted condition. (A) Predictions based on mRNA abundances. Results are shown for the SVM with radial kernel, which was the best performing model in the tuning process on mRNA data, where it won 55 of 60 independent runs. In this sub-figure, the average of the diagonal line is 60.5% and corresponding multi-class macro F_1 score is 0.61. (B) Predictions based on protein abundances. Results are shown for the SVM with sigmoidal kernel, which was the best performing model in the tuning process on protein data, where it won 41 of 60 independent runs. In this sub-figure, the average of the diagonal line is 55.1% and corresponding multi-class macro F_1 score is 0.56.

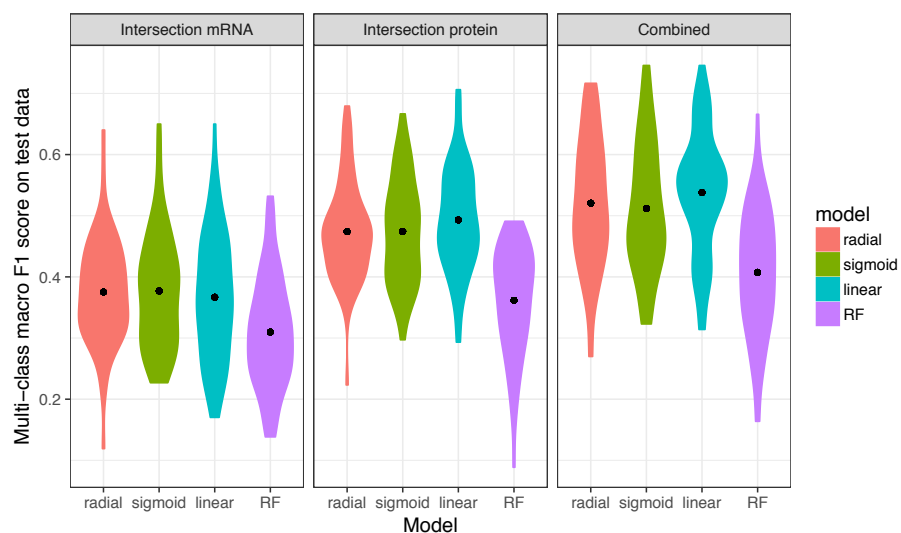
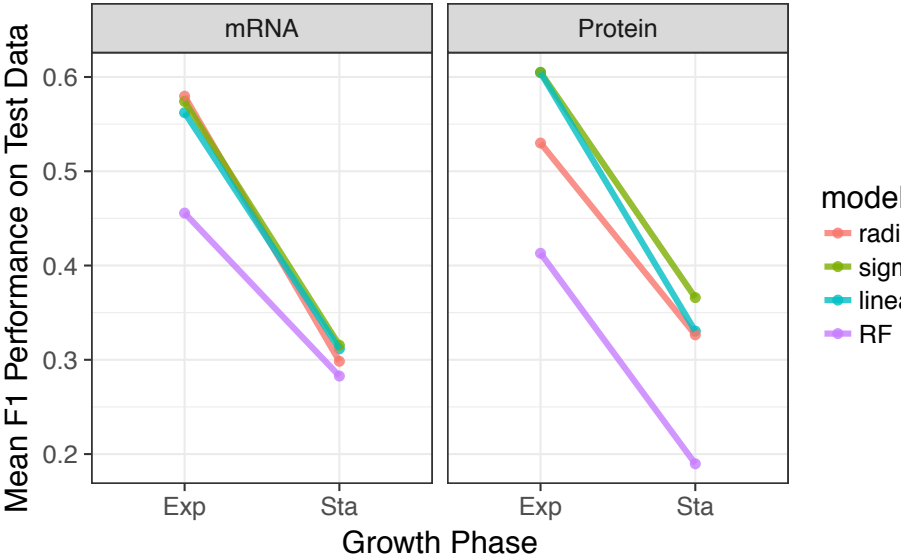


Figure 5. Models trained on both mRNA and protein data perform better than models trained on only one data type. The 102 samples for which we have both protein and mRNA abundances were used to compare the performance of machine learning models based on only mRNA, only protein, and mRNA and protein data combined (left to right, respectively). Regardless of the machine learning model used, prediction performance was higher for models that use protein data compared to mRNA data. Further, using both mRNA and protein data resulted in higher predictive power compared to either alone. Statistical significance of these differences is reported in Table 2.

|

1370



1371
1372
1373
1374
1375
1376
1377
1378

Figure 6. Prediction accuracy systematically declines from exponential to stationary. We separated data by growth phase and then trained [separate](#) models to predict carbon source, magnesium level, and sodium level within each growth phase. Regardless of [the](#) data source, prediction accuracy was substantially lower for stationary-phase samples than for exponential-phase samples. For each model and growth phase, dots show the mean F_1 score over 60 replicates and lines connect mean F_1 scores calculated for the same model.

Formatted: Header

Deleted: machine-learning model

Deleted: (mRNA or protein),

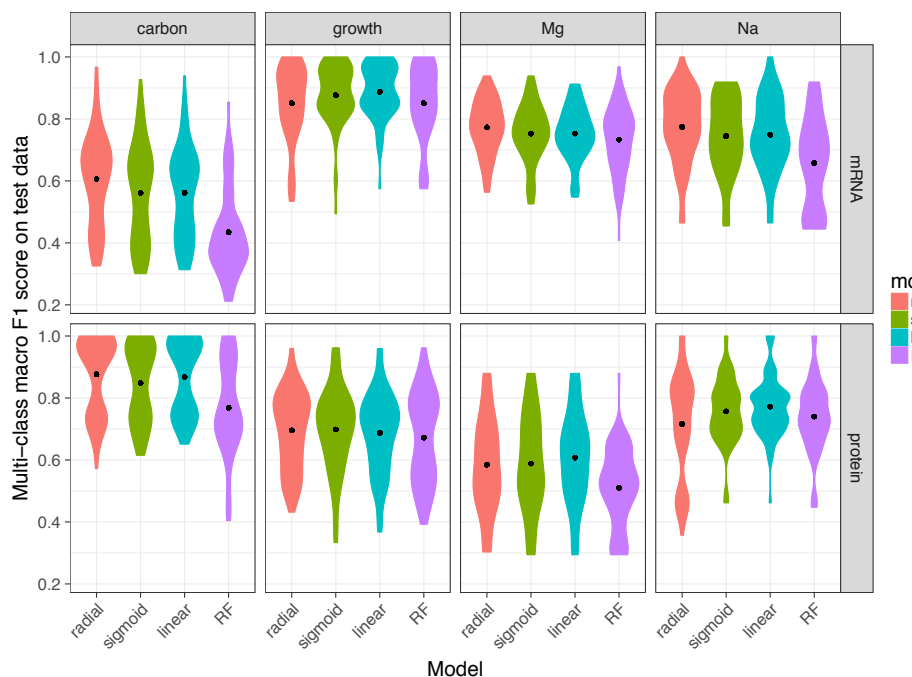


Figure 7. Model performance on univariate predictions. The multi-class macro- F_1 score of tuned models over test data for four individual conditions: carbon source, growth phase, Mg^{2+} levels, and Na^+ levels. To keep mRNA-based and protein-based predictions comparable, we used the 102 samples with both mRNA and protein abundances for this analysis. To facilitate comparison with our previous results, we used the multi-class macro- F_1 score even for univariate predictions by averaging the component F_1 scores for the individual outcomes (such as the different carbon sources).

Tables

Table 1: Winning-model distributions at the tuning stage. Numbers show the number of times out of 60 independent runs that each given model had the highest F_1 score in the tuning process. Results are shown separately for predictions on the mRNA and the protein data. The ties are counted for all the "winner" models as a result the sums are bigger than 60

Formatted: Header

Deleted:

Deleted: Note that

Deleted:

Deleted: ,

Deleted: ,

Deleted: .

Deleted: ¶

A

Sample	Na level	Mg le
A (Base)	base	high
B (Glycerol)	base	high
C (High Na)	base	high
D (Stationary phase)	base	base
E (Late stationary phase)	base	base

B

Sample	Na level	Mg le
A (Base)	base	base
B (Glycerol)	base	base
C (High Na)	high	base
D (Stationary phase)	base	base
E (Late stationary phase)	base	base

Figure 8.

Formatted: Level 2, Space Before: 10 pt, Line spacing: 1.5 lines, Keep with next, Keep lines together

Moved down [1]: **Performance of the protein model on external data.** For each of the five external samples we matched to conditions in our dataset, we show the predicted sodium level, magnesium level, carbon source, and growth phase.

Formatted: Font: Not Bold, Font color: Text 1

Deleted: Black text indicates a correct prediction. Red text indicates an incorrect prediction. Blue text indicates a prediction for a condition where the external data falls between two categories in our data (see Methods for details). (A) Predictions using a model trained on our complete dataset. Any missing protein abundances in the external test data were replaced by the median values from the training dataset. (B) Predictions using a model that was trained on our complete dataset using only the subset of proteins that were present in the external test data. ¶

Page Break

Formatted: Font: 13 pt, Bold

Formatted: Header

Model	mRNA	Protein
SVM, radial kernel	53	8
SVM, sigmoidal kernel	6	41
SVM, linear kernel	0	3
Random Forest	1	13

Table 2: Statistical significance of comparisons shown in Figure 5. Distributions of multi-class macro F_1 scores were compared using t-tests. The adjusted P value reports the false discovery rate (FDR). All comparisons are statistically significant after correction for multiple testing via FDR.

Model	Comparison	P value	Adjusted P value
SVM, radial kernel	mRNA vs protein	1.943E-09	4.663E-09
SVM, radial kernel	mRNA + protein vs mRNA	3.908E-13	2.345E-12
SVM, radial kernel	mRNA + protein vs protein	8.425E-03	1.087E-02
		3.327E-08	6.654E-08
SVM, sigmoidal kernel	mRNA vs protein		
SVM, sigmoidal kernel	mRNA + protein vs mRNA	3.088E-11	1.235E-10
SVM, sigmoidal kernel	mRNA + protein vs protein	3.517E-02	3.517E-02
		4.728E-11	1.418E-10
SVM, linear kernel	mRNA vs protein		
SVM, linear kernel	mRNA + protein vs mRNA	1.595E-15	1.914E-14
SVM, linear kernel	mRNA + protein vs protein	9.441E-03	1.087E-02
		1.818E-03	2.727E-03
Random forest	mRNA vs protein		
Random forest	mRNA + protein vs mRNA	1.928E-07	3.306E-07
Random forest	mRNA + protein vs protein	9.968E-03	1.087E-02

Table 3: Performance of the protein model on external data. For each of the five external samples we matched to conditions in our dataset, we show the predicted sodium level, magnesium level, carbon source, and growth phase. Regular text indicates a correct prediction for the sample in the given column, the \ddagger symbol indicates an incorrect prediction, and the \dagger symbol indicates a prediction where the external data falls between two categories in our data (see Methods for details). Predictions here are based on a model trained using our complete dataset, and any missing protein abundances in the external test data were replaced by the median values from the training dataset.

Moved (insertion) [1]

Formatted: Font: Not Bold, Font color: Text 1

<u>Sample</u>	<u>Na⁺ level</u>	<u>Mg²⁺ level</u>	<u>Carbon source</u>	<u>Growth phase</u>
<u>A (Base)</u>	<u>base</u>	<u>high[†]</u>	<u>Glucose</u>	<u>Exponential</u>
<u>B (Glycerol)</u>	<u>base</u>	<u>high[†]</u>	<u>Glucose[†]</u>	<u>Exponential</u>
<u>C (High Na⁺)</u>	<u>base[†]</u>	<u>high[†]</u>	<u>Glucose</u>	<u>Exponential</u>
<u>D (Stationary)</u>	<u>base</u>	<u>base</u>	<u>Glucose</u>	<u>Stationary</u>
<u>E (Late stationary)</u>	<u>base</u>	<u>base</u>	<u>Glucose</u>	<u>Stationary[†]</u>

Table 4: Performance of the protein model on external data with different missing value assumptions. Similar to Table 3, here we show the accuracy of predictions based on a model that was trained only on the subset of proteins from our dataset that were present in the external test data.

<u>Sample</u>	<u>Na⁺ level</u>	<u>Mg²⁺ level</u>	<u>Carbon source</u>	<u>Growth phase</u>
<u>A (Base)</u>	<u>base</u>	<u>base</u>	<u>Gluconate[†]</u>	<u>Exponential</u>
<u>B (Glycerol)</u>	<u>base</u>	<u>base</u>	<u>Gluconate[†]</u>	<u>Exponential</u>
<u>C (High Na⁺)</u>	<u>high</u>	<u>base</u>	<u>Glucose</u>	<u>Exponential</u>
<u>D (Stationary)</u>	<u>base</u>	<u>base</u>	<u>Glucose</u>	<u>Stationary</u>
<u>E (Late stationary)</u>	<u>base</u>	<u>base</u>	<u>Glucose</u>	<u>Stationary[†]</u>

Supporting information

S1 Table: Feature importance in principal component analysis. Listed are the top 10 genes that contribute the most to the indicated dataset and principal component.

S1 Fig. Tuning results for predictions based on mRNA data, generated from one of 60 independent runs and chosen for demonstration purposes. Model performance is measured as the mean F_1 score over 10 independent tuning runs. Higher numbers indicate better performance. (A) Tuning results for SVMs with linear kernel. Only the cost parameter was tuned. (B) Tuning results for SVMs with radial kernel. The cost and gamma parameters were tuned. The red dot indicates the winning parameter combination. (C) Tuning results for SVMs with sigmoidal kernel. The cost and gamma parameters were tuned. The red dot indicates the winning parameter combination. (D) Tuning results for random forest models. The mtry, nodesize, and ntrees parameters were tuned. We used three values for ntrees, 1000, 5000, and 10000, shown as three separate panels. The red dot indicates the winning parameter combination.

S2 Fig. Tuning results for predictions based on protein data, generated from one of 60 independent runs and chosen for demonstration purposes. (A) Tuning results for SVMs with linear kernel. Only the cost parameter was tuned. (B) Tuning results for SVMs with radial kernel. The cost and gamma parameters were tuned. The red dots indicate the winning parameter combinations. (C) Tuning results for SVMs with sigmoidal kernel. The cost and gamma parameters were tuned. The red dot indicates the winning parameter combination. (D) Tuning results for random forest models. The mtry, nodesize, and ntrees parameters were tuned. We used three values for ntrees, 1000, 5000, and 10000, shown as three separate panels. The red dot indicates the winning parameter combination.

S3 Fig. Percentage of correct predictions as a function of the number of samples during training. (A) Predictions based on mRNA abundances. (B) Predictions based on protein abundances.

S4 Fig. The error count distribution for mRNA (A) and protein (B) confusion matrices. The number of mis-predicted labels (x-axis) indicates how many of the 4 possible condition variables that an individual prediction got wrong. 0 mis-predicted labels (the majority in both cases) means that model predictions were 100% accurate. In both cases (mRNA and protein), when an incorrect prediction was made, it was most frequently due to a single variable being incorrectly predicted (number of mis-predicted labels with a value of 1) as compared to errors predicting more than one variable for a given condition (2 and 3 mis-predicted labels).

S5 Fig. Prediction accuracy for specific growth conditions for intersection mRNA data. Rows represent true conditions and columns represent predicted conditions. The numbers in the cells and the shading of the cells represent the percentage (out of 60

Formatted: Header

Formatted: Font: 12 pt, Font color: Auto

Formatted: None, Space Before: 0 pt, Line spacing: single, Don't keep with next, Don't keep lines together, Tab stops: 5.12", Left

independent replicates) with which a given true condition is predicted as a certain predicted condition. Predictions based on mRNA abundances, generated by using subset of mRNA samples which has matching protein pairs. Results are shown for the SVM with radial kernel, which was the best performing model in the tuning process on mRNA data, where it won 48 of 60 independent runs. In this figure average of the diagonal line is 44.1% and multi class macro F1 score is 0.43.

S6 Fig. Prediction accuracy for specific growth conditions for intersection protein data. Rows represent true conditions and columns represent predicted conditions. The numbers in the cells and the shading of the cells represent the percentage (out of 60 independent replicates) with which a given true condition is predicted as a certain predicted condition. Predictions based on protein abundances, generated by using subset of protein samples which has matching mRNA pairs. Results are shown for the SVM with sigmoid kernel, which was the best performing model in the tuning process on mRNA data, where it won 47 of 60 independent runs. In this figure average of the diagonal line is 52.3% and corresponding multi class macro F1 score is 0.53.

S7 Fig. Prediction accuracy for specific growth conditions for intersection mRNA & protein data. Rows represent true conditions and columns represent predicted conditions. The numbers in the cells and the shading of the cells represent the percentage (out of 60 independent replicates) with which a given true condition is predicted as a certain predicted condition. Predictions based on protein abundances, generated by using subset of mRNA & protein samples which has matching pairs. Results are shown for the SVM with sigmoid kernel, which was the best performing model in the tuning process on combined intersection data, where it won 27 of 60 independent runs. In this figure average of the diagonal line is 56.1% and corresponding multi class macro F1 score is 0.57.

S8 Fig. Prediction accuracy for univariate predictions using intersection mRNA and intersection protein data, as in the main text Figure 7. (A) Prediction of carbon source from mRNA abundances. (B) Prediction of carbon source from protein abundances. (C) Prediction of growth phase from mRNA abundances. (D) Prediction of growth phase from protein abundances. (E) Prediction of Mg^{2+} levels from mRNA abundances. (F) Prediction of Mg^{2+} levels from protein abundances. (G) Prediction of Na^+ levels from mRNA abundances. (H) Prediction of Na^+ levels from protein abundances.

S9 Fig. Prediction accuracy for univariate predictions based on intersection mRNA abundances, intersection protein abundances, or the combined dataset including both mRNA and protein abundances. Protein abundances are more predictive for carbon source and Mg^{2+} levels, and mRNA abundances are more predictive for Na^+ levels and growth phase.

Page 3: [1] Deleted	Hockenberry, Adam J	10/10/18 2:03:00 PM
Page 12: [2] Deleted	Hockenberry, Adam J	10/10/18 2:03:00 PM
Page 20: [3] Deleted	Hockenberry, Adam J	10/10/18 2:03:00 PM